Evaluating Human Electromagnetic Exposure in a Unmanned Aerial Vehicle (UAV)-aided Network

Thomas Detemmerman

Supervisor(s): Prof. dr. ir. Wout Joseph, Prof. dr. ir. Luc Martens

Abstract—Society relies more than ever on the availability of wireless networks. Due to the mobility of a UAV, a UAV-aided network is able to provide this necessary access in case the existing terrestrial network gets damaged. However, the public is concerned about the potential health effects of the electromagnetic radiation caused by these networks. Therefore, mobile devices and base stations have to comply to strict legislation enforced by the government.

This research investigates how different scenarios influence power consumption, electromagnetic exposure and specific absorption rate. These different scenarios are defined by various flying heights, number of UAVs available and population densities. Further, also an analysis on the difference between a realistic microstrip patch antenna and a fictional equivalent isotropic radiator is performed. Thereafter, the network will be optimized towards goals like electromagnetic exposure of the average user or power consumption of the entire network which result in conflicting requirements.

To accomplish this goal, a capacity based deployment tool will be used which simulates an entire UAV-aided network. In this way, all important sources for electromagnetic radiation, like all user equipment and all flying base stations, will be considered.

It looks from the results that a power consumption optimized network with a fixed flying height of 80 metres is the recommended approach for the city centre of Ghent. A microstrip patch antenna with a sufficiently large aperture angle is a good starting point. However, different antenna array configurations still have to be investigated.

Keywords— LTE, microstrip patch antenna, radiation pattern, specific absorption rate (SAR), deployment tool, electromagnetic exposure, power consumption, wireless access network, emergency network, UAV, unmanned aerial base stations

I. Introduction

SOCIETY is constantly getting more and more dependent on wireless communication. On any given moment, in any given location, an electronic device can request to connect to the bigger network. Devices need more than ever to be connected, starting from small Internet of Things (IoT) up to self-driving cars which all need to be supported by the existing infrastructure.

Also in exceptional and possibly life threatening situations, the public relies on the cellular network. One solution for a fast temporarily deployable network is with the usage of a UAV. A base station can be attached to these flying UAVs to support the damaged network over a limited area. This approach is also useful in case of an unexpected increase in traffic. For example during the terrorist attacks at Brussels Airport, mobile network operators saw all telecommunications drastically increasing causing moments of contention. Some operators even decided to temporarily exceed the exposure limits in order to handle all connections [1]. Electromagnetic exposure can however not be neglected. Research shows how excessive electromagnetic radiation can cause diverse biological side effects [2], [?]. It becomes clear that electromagnetic exposure

is a key value when designing a UAV-aided network and should definitely not surpass the limits predefined by the government.

UAV-aided networks can, thanks to their mobility, easily be repositioned towards a certain goal. Several papers explain how a network can be optimized towards different goals like power consumption. However, very limited research has been done where a UAV-aided network is optimized towards electromagnetic exposure. While several publications exist, discussing how the electromagnetic exposure can be calculated. Most of them only consider a limited number of sources like only base stations or only mobile phones. Papers who cover electromagnetic exposure from all the different sources and convert it into a single value are rather limited.

This research proposes a method to optimize the network towards electromagnetic exposure and power consumption when considering all four sources of radiation in a telecommunications network, being: the user's own phone, the base station that is serving this user, all devices from other users in the network and all other active base stations that are not serving this user. In this way, the contribution of each source towards the total electromagnetic exposure can easily be identified.

The behaviour of the electromagnetic exposure and power consumption of the network will be analysed by applying the tool in different scenarios like different types of antennae and various flying height and population densities. Values like Specific Absorption Rate (SAR), electromagnetic exposure and power consumption will give insight in how the network behaves so the network could be optimized accordingly.

To make this research possible, an existing capacity based deployment tool developed by the WAVES research group at Ghent University is used. This planning tool describes a fully configured UAV-network which is a suitable starting point for this research.

II. State of the Art

A. Electromagnetic exposure

Users in a telecommunication network are exposed to various sources of electromagnetic radiation, expressed in V/m. Once this exposure is absorbed by the human body we are talking about specific absorption rate (SAR) and is expressed in W/kg. All these values are subjected to limitations enforced by the government. This research is done in Ghent, a Flemish city in Belgium, where in the 2.6

GHz frequency band, an individual antenna cannot exceed 4.5 V/m and the cumulative sum of all fixed sources has its maximum at 31 V/m [3], [?]. The maximum SAR-values for the whole body over a 10 g tissue (SAR_{10g}) is $2W/kg$ [4].

Several papers calculate exposure originating from certain sources [5], [?], [?], [?] where some convert the uplink (UL) radiation into localized specific absorption rates [?], [?]. With the advent of 5G, paper [6] describes how the localized SAR-values are achieved from different sources. Finally, [7] describes how both UL and downlink (DL) traffic can be converted into a single whole body SAR value.

In a realistic network, some users are calling while others are using other types of telecommunication services like browsing the web. Therefore, all absorbed electromagnetic exposure should be expressed in whole body SAR while still covering all sources.

B. Optimized UAV-aided networks

A UAV knows several applications. It was originally mainly used to support the military for surveillance and remote attacks without endangering pilots [8]. However, UAVs have recently become more accessible by the general public due to decreasing costs. This allowed UAVs to be researched for various applications.

A UAV equipped with a femtocell base station antenna will be called a Unmanned Arial Base Station (UABS) which brings several advantages like mobility and rapid deployment. However, it brings also challenges like limited weight of the payload and sparse power supply.

Kawamoto et al. introduced in [9] a WiFi network with the support of UAVs while considering resource allocation and antenna directivity. Gangula et al. illustrates in [10] how UAVs can be used as a relay for LTE. Zeng et al. proposes in [8] a tutorial in 5G-and-beyond wireless systems where challenges like energy consumption, mobility and antenna direction are discussed. Deruyck et al. designed in [11] a capacity based deployment tool for UAV-aided emergency networks for large-scale disaster scenarios where an ideal flying height of 100 m is suggested. This was expanded in [12] with a performance evaluation of the direct-link backhaul of this tool where a slightly lower flying height of 80 metres is recommended.

Mozaffari et al. provides in [13] guidelines on how to optimize and analyse UAVs equipped for wireless communication equipment. One path that has been excessively researched are location optimization solutions where the network is designed in such a way that certain goals like minimal power consumption are achieved [14], [15], [16], [17]. These optimizations can be achieved through different implementation methods like exact algorithms or machine learning [13], [18].

Research where network is optimized towards electromagnetic exposure is rather limited. Deruyck et al. discusses in [19] how a terrestrial network can be optimized towards either a minimal exposure or minimal power consumption of the entire network. However, to the best of the author knowledge, no research has been done where a UABS-network has been optimized towards electromagnetic exposure.

C. Technologies

For the deployment of the network, the more robust UAVs from [11] will be used and will be operating in the 2.6 Ghz bandwidth. Since the users are assumed to experience a constant electromagnetic exposure without interruptions, frequency division duplex is used.

The onboard antenna of the UAV will act as the gateway between the UE and the backhaul network. However, determining which antenna to use and how to position it, can be challenging. The radiation pattern from the antenna can be influenced by the UAV [20]. Also the fact that the UAV will hover above the user makes tradional 2D modelling insufficient. A 3D-model which accounts for both elevation and azimuth directivity will be required [8].

The easiest radiation pattern is a hypothetical isotropic radiator which radiates equally in all directions. Antennae that radiate equal quantities for a certain plane are called omnidirectional antennae [8] and several types have been investigated for UAV usage like monopoles, dipoles and wing antennae have been considered [21], [22], [23], [24]. Another type of antennae are directional antennae. One type that has excessively been researched in various array-configurations are microstrip patch antennae [25], [26], [27]. They provide several advantages compared to traditional antennae [28], [?] like lightweightness, low in cost and thin causing them to be more aerodynamic.

A basic microstrip antenna consists of a ground plane and a radiating patch, both separated with a dielectric substrate. Several variations exist like microstrip patch antenna, microstrip slot antenna and printed dipole antenna which all have similar characteristics [28], [?]. They are all thin, support dual frequency operation and they all have the disadvantage that they will transmit at frequencies outside the aimed band which is also known as spurious radiation. The microstrip patch and slot antenna support both linear and circular polarization while the printed dipole only supports linear polarization. Further is the fabrication of a microstrip patch antenna considered to be the easiest of the considered patch antenna [28].

III. Scenarios

The default configuration is given below and is always applicable unless mentioned otherwise.

Four possible configurations will be investigated in different scenarios. There are two possible antennae, namely EIRP and microstrip pach antenna, which can both be applied in a power consumption optimized network or an exposure optimized network.

Three main scenarios will be investigated. First, only one user with one drone will be present in the network. SAR, electromagnetic exposure, power consumption and antenna transmission power are investigated at different flying heights.

In a second scenario, the network is expanded for multiple users but with still only one drone available. The

Broadband cellular network	
technology	LTE
frequency	2.6 GHz
Carrier	
carrier power	13.0 A
average carrier speed	12.0 m/s
average carrier power usage	17.33 Ah
carrier battery voltage	22.2 V
Femtocell antenna	
maximum P_{tx}	33 dBm
antenna direction	downwards (az: 0°; el: 90°)
gain	4 dBm
feeder loss	2 dBm
implementation loss	0 dBm
radiation pattern	EIRP or microstrip patch
height	100m
UE Antenna	
height	1.5m from the floor
gain	0 dBm
feeder loss	0 dBm
radiation pattern	EIRP
number present in the network	224

TABLE I

Overview of default configuration values.

		Optimization strategy	
		Exposure optimized	Power consumption optimized
Antenna type	Equivalent isotropic radiator	EIRP, Exp Opt	EIRP, PwrC Opt
	Microstrip patch antenna	Microstrip, Exp Opt	Microstrip, PwrC Opt

Fig. 1

Matrix with the four possible configurations

scenario is divided into two cases. One with a variable flying height but with a fixed number of 224 users which is an average day at 5 p.m. in Ghent. In the other case, the number of users varies but the flying height is set to 100 [11]. The power consumption, electromagnetic exposure and specific absorption rate are investigated in the four different configurations.

The third scenario is quite similar to the previous scenario. It has the same two cases with each its four config-

urations. The only exception is that an unlimited number of UABSs are available.

IV. Methodology

A. Electromagnetic Exposure

The total whole body SAR ($SAR_{10g}^{wb,total}$) (expressed in W/kg) of a user can be calculated by a simple sum of individual SAR values from the different sources and is based on [6] where SAR values are used that are induced into the head. Using SAR_{10g}^{head} would however result into incorrect conclusions since the position of the phone relative to the user is unknown. The position of the phone can be next to the head but also in front of the user. The induced electromagnetic radiation will therefore be expressed in function of the entire body.

$$SAR_{10g}^{wb,total} = SAR_{10g}^{wb,my\_UE} + SAR_{10g}^{wb,my\_UABS}$$
$$+ SAR_{10g}^{wb,other\_UE} + SAR_{10g}^{wb,other\_UABSs} \quad (1)$$

The first parameter, SAR_{10g}^{wb,my_UE}, indicates the absorbed electromagnetic radiation by the whole body originating from the user's own device. However the UL radiation is destined for the serving UABS, a portion of that radiation is directly absorbed by its user, due to the omnidirectional nature of the mobile antenna. The second parameter, SAR_{10g}^{wb,my_UABS}, represents the DL radiation caused by the UABS who is serving the user. As the third parameter, we have the $SAR_{10g}^{wb,other\_UE}$ which is radiation caused by the device of other people. The radiation of these devices is once again destined for a specific UABS but again, a portion of that UL radiation will also be absorbed by our user. Finally, $SAR_{10g}^{wb,other\_UABSs}$ represents the DL radiation by the other UABSs to which our user is exposed to but not served by. An illustration is given in figure 2 where the green arrow is a type near-field radiation while the others represent far-field radiation.
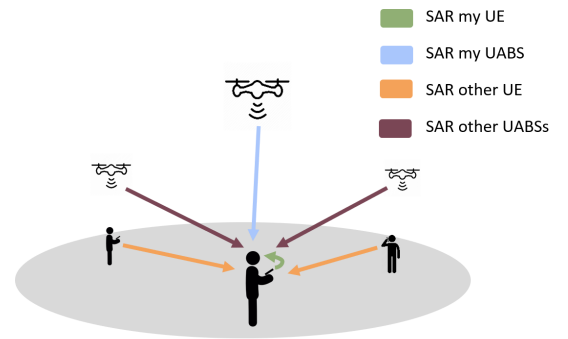

Fig. 2

Illustration of the network that shows how the average user (here shown in the center) is influenced by different types of sources.

B. Electromagnetic Exposure Caused by Far-Field Radiation

B.1 Electromagnetic Radiation from a Single Source

Calculating far-field exposure needs to be done for all UABSs and UE that do not belong to the user. To determine the total exposure E (expressed in V/m) of this single user u from a single radiator i can be calculated as follows.

$$E_i(u)[V/m] = 10^{\frac{RRP(u)[dBm]-43.15+20*\log(f[Mhz])-PL(u)[dB]}{20}}$$ (2)

Caculating the real radiation power (RRP) for a certain user u, requires first the EIRP-value to be calculated [5], [?]. This is achieved by adding the transmit power P_t to the transmitter gain G_t and thereafter subtracting the feeder loss L_t. This formula needs to be expanded to also account for attenuation. This value depends on the angle between this user and the antenna's main beam. This leads to the following formula.

$$RRP[dBm] = P_t[dBm] + G_t[dBi] - L_t[dB] \\ -attenuation(u)[dB]$$ (3)

The used frequency in formula 2 is denoted as f and is expressed in MHz. Since LTE is used, this value will be 2600 MHz.

At last, formula 3 requires the path loss (in dB). In order to calculate this, an appropriate propagation model -of which several exist- is required . The Walfish-Ikegami model is used since it performs well for femtocell networks in urban areas [11].

B.2 Combining Exposure

The electromagnetic exposure, in a certain spot, originating from different sources can be calculated with formula 4. E_i stands for the electromagnetic exposure from source i and n stands for all far-field radiators of a certain category which will either be UABSs or UE from other people. E_{tot} will be calculated for each location where a user is positioned.

$$E_{tot}[V/m] = \sqrt{\sum_{i=1}^{n}(E_i[V/m])^2}$$ (4)

B.3 Converting electromagnetic radiation into SAR-values

Formula 1 expects that the radiation is expressed in whole body SAR. To make this calculation possible, a distinction has to be made between near-field SAR $SAR^{wb,nf}$ and far-field SAR $SAR^{wb,ff}$.

Converting the electromagnetic radiation is done with a conversion factor which is based on Duke of the Virtual Family. Duke is a 34-year old male with a weight of 72 kg, a height of 1.74 m and body mass index of 23.1 kg/m [7]. Research shows that the conversion factor for WiFi in the far-field is $0.0028 \frac{W/kg}{W/m^2}$ and for $0.0070 \frac{W/kg}{W}$ [7] in the near-field.

Since WiFi, at a frequency of 2400 MHz, is very close to LTE, at 2600 MHz, is very close to LTE, at 2600 MHz, it is assumed in [7] that this value is also applicable for Long-Term Evolution (LTE).

Caculating SAR from far-field radiation is done as follows:

$$S[W/m^2] = \frac{(E_{tot}[V/m])^2}{337}$$ (5)

$$SAR_{10g}^{wb,ff}[W/kg] = S[W/m^2] * 0.0028 \left[\frac{W/kg}{W/m^2}\right]$$ (6)

The constant in 6 converts the power flux density S to the required $SAR_{10g}^{ff,wb}$. To make this possible, the electromagnetic radiation from formula 4 should first be converted to the power flux density with formula 5.

The SAR caused by near-field radiation is calculated by multiplying the constant with the used transmission power of the User Equipment (UE) (eq. 7) as follows:

$$SAR_{10g}^{wb,nf}\left[\frac{W}{kg}\right] = 0.0070 \left[\frac{W/kg}{W}\right] * P_{tx}[W]$$ (7)

C. Microstrip Patch antenna

A microstrip patch antenna is chosen because it allows easy production but more important, it has a low weight and has a thin profile causing it to be very aerodynamic which is useful when attaching it to a drone [28].

The dimensions of the antenna depend on the frequency it is operating at and the characteristics of the used substrate. The antenna will be radiating at a centre frequency f_0 of 2.6 GHz. Each substrate has a dielectric constant ϵ_r representing the permittivity of the substrate and depends on the used material. Substrates with a high dielectric constant and low height reduce the dimensions of the antenna while a lower dielectric constant with a high height improves the performance of the antenna. In this document, a substrate like glass is chosen because of the higher dielectric constant of $\epsilon_r = 4.4$ compared to materials like teflon with only a dielectric constant of $\epsilon_r = 2.2$ [29]. Doing this in combination with an antenna height of 2.87 mm will decrease the dimensions of the entire antenna surface. This comes in handy since drones only have limited space available.

description	symbol	value
centre frequency	f_0	2600 Hz
dielectric constant	ϵ_r	4.4
height of the substrate	h	0.00287 m

TABLE II

Overview of configuration parameters.

The dimensions of the radiating patch can be calculated with the formulas from [29], [?]. Doing so will result in a radiating patch of 35.09 mm by 26.55 mm and a groundplane of at least 52.40 mm by 43.80 mm. The microstrip patch antenna as illustrated in fig. 3 will result in the radiation pattern of fig. 4.
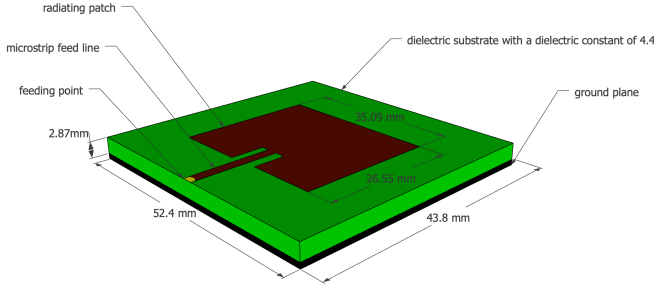
Fig. 3
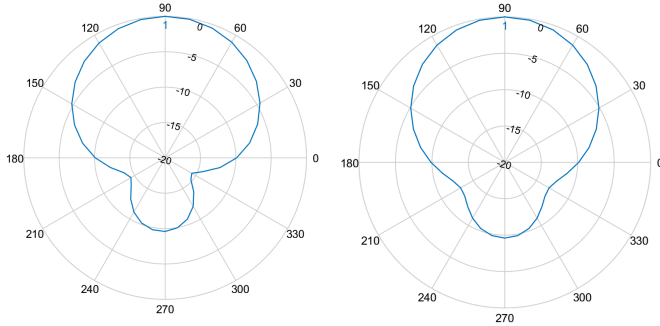Design of the microstrip patch antenna.

Fig. 4
Radiation pattern 1: On the left the radiation pattern of the E-plane and at the right for the H-plane.

D. Optimizing the network

Margot et al. discusses in [19] how a terrestrial telecommunication network either can be optimized towards electromagnetic exposure of an individual or towards power consumption of the entire network. However an increasing transmission power of an antenna comes with an increasing electromagnetic exposure. This is not the case considering both values for an entire network. In fact, the authors from [19] prove that both become inversely equivalent. The reason the network behaves like this is because it is often cheaper to increase the exposure of an already active base station than activating a new one. This leads to the following fitness function which is based on [19].

$$ f = w * \left(1 - \frac{E_m}{E_{max}} \right) + (1 - w) * \left(1 - \frac{P}{P_{max}} \right) * 100 \quad (8) $$

Formula 8 returns a fitness value which represents the performance of the entire network. w is the importance factor of electromagnetic exposure ranging from 0 to 1, boundaries included. A w set to zero means that electromagnetic exposure is not important. Such a network will therefore be called a power consumption optimized network. Likewise, a w set to one means that minimizing exposure is top priority and will result in an exposure optimized network. P_{max} is the power consumption of all

UABSs, both active and inactive, when radiating at the highest level possible while P is the effective power used by the current designed network. This will be the power required for the flying drones themselves and their antennae. E_m will be the weighted exposure of the average user for the current designed network and E_{max} the weighted average electromagnetic exposure when all antennae are at their highest power level.

When optimizing the network, it is not only important to consider the average exposure of all users, but also to limit high extremes [19]. A weighted average will be used not only considering the median but also the 95 percentile from all users' DL exposure using formula 9. Since both values are considered to have equal importance, the weight factors w_1 and w_2 will both have an equal importance of 50%.

$$ E_m = \frac{w_1 * E_{50} + w_2 * E_{95}}{w_1 + w_2} \quad (9) $$

V. Results

A. One User and One UAV

The results show that for a varying flying height, a logarithmic relationship exists between the P_{tx} and the flying height. This is mainly caused by the logarithmic scale in which the decibels of the P_{tx} are expressed. So while 10 dBm equals 10 mW, 20 dBm equals 100 mW. Each time the flying height becomes too large to cover, the P_{tx} increases with one dBm. When using the default configuration where the maximum allowed P_{tx} is set to 33 dBm, a UABS can fly up to 387 m before losing connection in a free line of sigh (LOS) scenario.

This scenario is investigated with a microstrip patch antenna using power consumption optimization. However, the chosen optimization strategy doesn't really matter because the decision algorithm decides which user needs to be connected to which UABS. Since only one UABS is available, both optimization strategies will behave identical. Further, also the used antenna will not make any difference. The user is namely positioned in the perfect centre of the main beam where there is no attenuation experienced for both antennae.

When investigating this scenario at different flying heights, we notice that the UL radiation increases exponentially while the DL radiation remains constant during the entire time. The reason that the DL radiation remains constant is because of power control which makes sure that no more power is used than strictly necessary. So at lower flying altitudes, there is less path loss and the UABS will therefore reduce the P_{tx}. This results in formula 10 where the electromagnetic exposure is a constant fraction of power and distance. The UL radiation starts very low but surpasses the DL radiation around 80 metres.

$$ \vec{E}(V/m) = \frac{\Delta U(V)}{\Delta x(m)} \quad (10) $$

B. Increased Traffic with one UABS

B.1 Variable Flying Height

A power consumption optimized network has the highest exposure, a behaviour that was already proven by [19]. However, a power consumption optimized network will have higher power consumption than an exposure optimized network. To understand this, the behaviour of the deployment tool needs to be understood first. A power consumption optimized network will result in a few high powered UABSs because increasing the input power of an antenna costs less than activating a new UAV. Likewise, an exposure optimized network generates a lot of low powered UABSs because the lower the power of the antenna, the lower the exposure. This has the consequence that the cover radius is less and therefore requires more UAVs which costs more energy. When only a limited amount of UABSs are available, like only one in this scenario, the tool will only keep UABSs which cover the most users. Therefore, the power consumption in a power consumption optimized network is much more higher.

Further, the results also show that the exposure increases with higher flying altitudes. At low flying altitudes, there is a lot of path loss by obstructing buildings. When UABSs fly higher, the exposure increases and more users become covered. The increasing electromagnetic radiation is however not unlimited. At even higher flying altitudes, the distance between a given UABS and users further away becomes too large causing the coverage to decrease again. When this decrease occurs depends on the configuration. A power consumption optimized network tends to decrease earlier than an exposure optimized network.

When replacing the fictional equivalent isotropic radiation power (EIRP) antenna by a microstrip patch antenna, the percentage of covered users drops for both optimization strategies. This is because users, who have a higher horizontal distance between themselves and the UABS, experience a higher attenuation.

The results further show that the radiation from the UABS is the main factor followed by the near-field radiation from the user's own device. The far-field radiation from other UE barely contribute anything.

B.2 Variable Number of Users

Also these results show how EIRP antennae designs are able to cover more users than microstrip patch antennae just like power consumption optimized networks will reach more users than exposure optimized networks. The contribution to the total SAR from each individual source is identical to the previous scenario. « deze zin weg?

There is still only one UABS available. So when population grows, more users become uncovered and therefore the average electromagnetic exposure decreases. For example, an EIRP power consumption optimized network will have the highest exposure and therefore covers the most users as opposed to a microstrip patch antenna in an exposure optimized network which will radiate the least and thus has the lowest number of covered users.

While the population grows, more and more users become uncovered causing the average SAR to drop. However, this does not conclude that by increasing the population, the SAR of a user who is directly beneath a UABS would be less. To investigate this, a user is positioned in the middle of the city centre of Ghent and a UAV is positioned above him. Initially, only 49 people are active around him. The SAR of our central user is monitored while the population around him is growing. Figure 5 shows with the black lines which users are connected. The left map is for only 50 users and shows that only one user is connected besides our central user. The map on the right is taken with 600 users and shows much more connected users. The results show how the UL SAR remains constant. A normal behaviour since the flying altitude does not change. The SAR from the UABS experiences a slight increase. When the population grows, more users become available and some will spawn near the central user. The UABS will likely decide to cover these users as well as visible in figure 5. These users might have a slightly worse path loss because of obstructing buildings or somewhat bigger distance. The UABS reacts to this by increasing his power consumption causing an increase in the DL SAR for the central user. The results further also show that the SAR from other UE increases when the population increases. But as mentioned before, it is much less compared to the other sources.
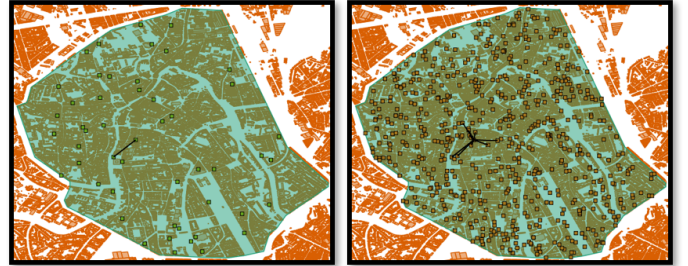

Fig. 5

Overview of which users are connected to the UABS. The map on the left is for 50 active users while the map on the right is with 600 active users.

C. Unlimited Number of UABSs

C.1 Variable Flying Height

The same scenario as the previous one is investigated. Only now, an unlimited number of UABSs is available. The results prove that the different optimization strategies work as intended. Power consumption optimized networks have indeed a lower power consumption but therefore result in higher electromagnetic radiation. On the other hand, an exposure optimized network will reduce the electromagnetic exposure by using more UAVs and thence also increase the network's power consumption. This conclusion was already made in [19] and is supported by these results.

The exposure in an exposure optimized network increases logarithmically while the power consumption op-
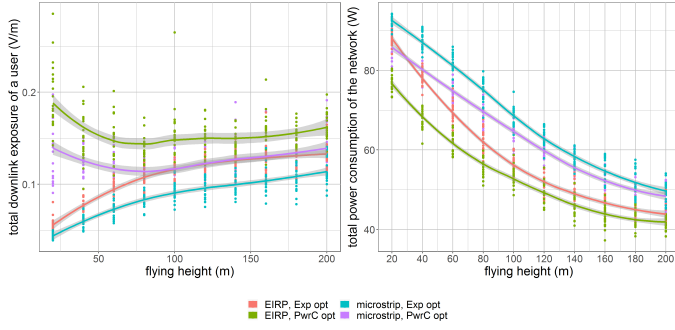
Fig. 6

These two figures show how the flying height influences the downlink electromagnetic radiation of the average user (left) and power consumption of the entire network (right) for an unlimited number of drones.

Fig. 7

Each chart corresponds with one of the four possible configurations. The contribution of each source towards the total SAR for a varying flying height is shown.

timized network rather shows a concave relationship with its lowest point at around 70 metres. At a flying height of 20 m, the exposure optimized network has on average 220 to 224 UABSs. That is (almost) one UABS for each user so it's logical that the electromagnetic exposure is very low. The number of UAVs in a power consumption optimized network is much less in order to save energy but the same percentage of coverage is still achieved. So these UAVs will try to cover more users requiring higher levels of radiation. This is certainly the case since there are a lot of obstructing buildings at this flying altitude. Because of this, users who are close and in LOS will experience much more electromagnetic radiation.

The results further show that the network profits from increasing the flying altitude. Not only less UAVs are needed but also the power consumption is lower. Both can be explained by the lower path loss when UABSs fly higher. At higher flying altitudes, the exposure from the UE increases. A behaviour also explained in the first scenario. The SAR from the serving UABS is identical to the exposure which has been explained earlier. When looking at the exposure from 'other UABSs', an increase in electromagnetic radiation at higher flying altitudes is noticed. Also here the lower path loss from less obstructing buildings will be the reason. The figures from 7 further also clearly show that this increase in electromagnetic radiation will be less for a microstrip patch antenna. The reason behind this is that energy will be more focussed towards the ground and there is less sideways radiation because of attenuation.

C.2 Variable Number of Users

When the flying height of the UABSs are fixed to 100 metres and the density of the population increases, also the number of required drones increases in order to reach a 100 % coverage. When the number of drones increases, so does the electromagnetic exposure and power consumption. Once again, the EIRP antenna in a power consumption network has the highest exposure for the lowest power consumption and a microstrip patch antenna in an expo-
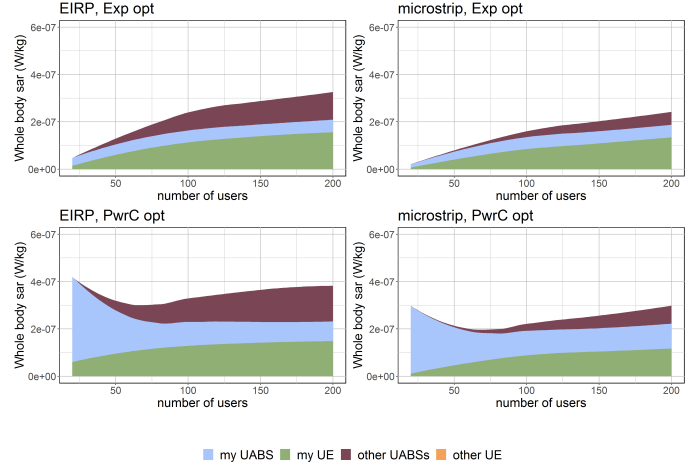
sure optimized network the lowest exposure for the highest power consumption. The two other combinations are in the middle and behave very similar.
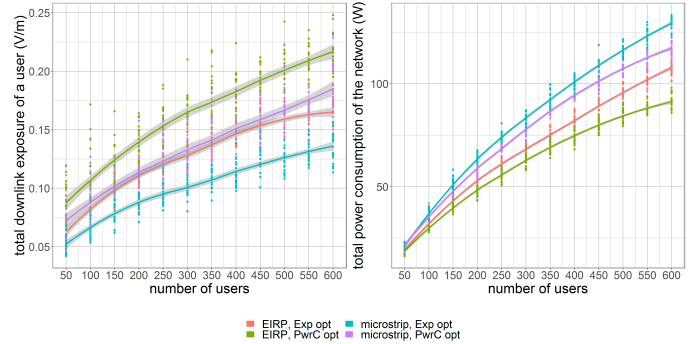

Fig. 8

These two figures show how the number of users influences the downlink electromagnetic radiation of the average user (left) and power consumption of the entire network (right) for an unlimited number of drones.

When looking at the different contributions to the total SAR in figure 9, we see that the weighted average SAR from the users' own device and from the serving UABS remains constant. The flying altitude is always the same so also the required energy to cover that distance will remain the same. The only SAR value that increases are the DL SAR from other UABSs and the UL SAR from other UE. When more users come online, also more UAVs will be radiating. Moreover, there is very little path loss because the flying height is above the average building.
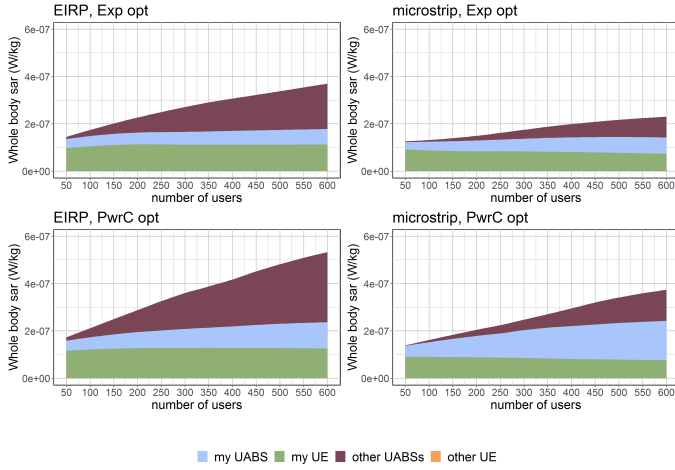
Fig. 9

Each chart corresponds with one of the four possible configurations. The contribution of each source towards the total SAR for a varying number of users shown.

VI. Conclusion

Literature showed that a network can be optimized towards either the power consumption of the entire network or the electromagnetic exposure of the average user using a fitness function [19]. However, the fitness function should be used with care considering that UABSs can be placed anywhere as opposed to the transmission towers from [19] who have a predetermined position. This causes that in an exposure optimized network, a lot of users get a UABS all by themselves because this is the best approach to minimize exposure. A power consumption optimized network on the other hand will try to limit the number of drones in order to save energy. So as a rule of thumb: an exposure optimized network will result in a lot of low powered devices (increasing the overall power consumption) while a power consumption optimized network results in a few high powered devices (increasing the exposure of the average user). If the goal is to remain in the air for a longer period of time, an exposure optimized network is recommended because the power consumption of an individual UABS is lower. On the other hand, a power consumption optimized network is cheaper because less drones are involved. Moreover, the results show that the electromagnetic radiation in a power consumption optimized network (with high powered UABSs) is far below the thresholds enforced by the Flemish government.

The user's main sources of exposure are the user's own device and the UABS who is serving him followed by all other UABSs in the network. When the population increases, there is not only more radiation from UE but also from more UABSs that are serving the other users. The exposure from other people their UE is so low that it can be neglected. An exposure optimized network will limit the total exposure mainly by trying to reduce the exposure

from other UABSs.

A directional microstrip patch antenna is introduced because it gives several advantages compared to omnidirectional antennae. Directional antennae are able to focus their energy there where it is needed, namely towards the ground. Microstrip patch antennae further benefit from their thin and lightweight design. The performance of this directional microstrip patch antenna has been compared to a fictional equivalent isotropic radiator. This equivalent isotropic radiator has higher exposure and coverage for less power, compared to realistic antennae like microstrip patch antennae because of the absence of attenuation, and can hypothetically be compared with an antenna with a very big aperture angle. This type of antenna can achieve the same coverage with less resources like power and number of drones. A microstrip patch antenna with a more limited aperture angle of 90° requires more resources but causes less sideways radiation. So the exposure from other UABSs will be way less.
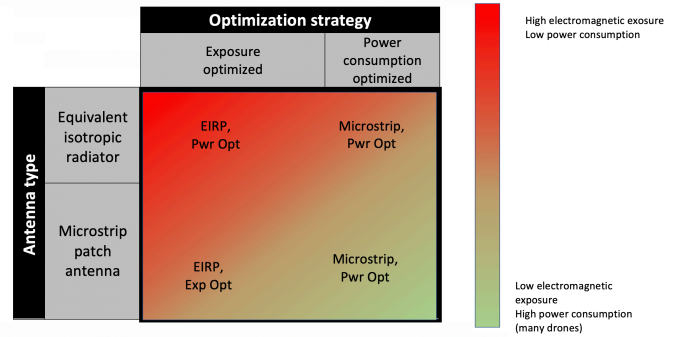

Fig. 10

Matrix with the four possible configurations. Colour-coded based on the results.

Remarkable is that an EIRP exposure optimized network behaves very similar to a microstrip power consumption optimized network as shown in figure 10. This results in the best of both worlds. The microstrip patch antenna will generate less electromagnetic radiation by design and the power consumption optimization reduces the number of required drones and power. A microstrip patch antenna with an aperture angle of 90° is considered as a good solution but if budget is limited, an antenna with a larger aperture angle would further reduce cost without interfering with the Flemish legislation regarding electromagnetic exposure.

The electromagnetic radiation of an exposure optimized network increases with higher flying altitudes. Around 80 metres, the exposure from the user's device surpasses the exposure from the serving UABS. On the other hand, a power consumption optimized network shows that the lowest exposure is measured around 70 to 80 metres. Further, the results also show that the number of required drones decreases when the flying height becomes larger. A conclusion that was also made in [11]. When also considering the

results from [12] where a flying altitude from 80 metres is suggested for an optimal access and backhaul connectivity, a flying height of 80 metres is also here proposed for the city centre of Ghent.

In short, a power consumption optimized network is proposed with a fixed flying height of 80 metres. A microstrip patch antenna with a sufficiently large aperture angle is a good starting point. However, different antenna configurations should be investigated.

Acknowledgement

References

[1] "Base overschreed stralingsnormen na aanslagen," De standaard, 2019.

[2] L. Hardell and C. Sage, "Biological effects from electromagnetic field exposure and public exposure standards," Biomedicine and Pharmacotherapy, vol. 62, no. 2, pp. 104 – 109, 2008.

[3] "Elektromagnetische velden en gezondheid: Uw wegwijzer in het elektromagnetische landschap," Federale overheidsdienst: volksgezondheid, veiligheid van de voedselketen en leefmilieu, vol. 5, 2014.

[4] E. Commission, "Council recommendation of 12 july 1999 on the limitation of exposure of the general public to electromagnetic fields (0 hz to 300 ghz)," Official Journal of the European Communities, vol. 59, 1999.

[5] D. Plets, W. Joseph, K. Vanhecke, and L. Martens, "Exposure optimization in indoor wireless networks by heuristic network planning," Progress In Electromagnetics Research, vol. 139, pp. 445–478, 01 2013.

[6] S. Kuehn, S. Pfeifer, B. Kochali, and N. Kuster, "Modelling of total exposure in hypothetical 5g mobile networks for varied topologies and user scenarios," Final Report of Project CRR-816, Available on line at: https://tinyurl. com/r6z2gqn, 2019.

[7] D. Plets, W. Joseph, K. Vanhecke, G. Vermeeren, J. Wiart, S. Aerts, N. Varsier, and L. Martens, "Joint minimization of uplink and downlink whole-body exposure dose in indoor wireless networks," BioMed research international, vol. 2015, 2015.

[8] Y. Zeng, Q. Wu, and R. Zhang, "Accessing from the sky: A tutorial on uav communications for 5g and beyond," Proceedings of the IEEE, vol. 107, no. 12, pp. 2327–2375, 2019.

[9] Y. Kawamoto, H. Nishiyama, N. Kato, F. Ono, and R. Miura, "Toward future unmanned aerial vehicle networks: Architecture, resource allocation and field experiments," IEEE Wireless Communications, vol. 26, no. 1, pp. 94–99, 2018.

[10] R. Gangula, O. Esrafilian, D. Gesbert, C. Roux, F. Kaltenberger, and R. Knopp, "Flying rebots: First results on an autonomous uav-based lte relay using open airinterface," in 2018 IEEE 19th International Workshop on Signal Processing Advances in Wireless Communications (SPAWC), pp. 1–5, IEEE, 2018.

[11] M. Deruyck, J. Wyckmans, W. Joseph, and L. Martens, "Designing uav-aided emergency networks for large-scale disaster scenarios," EURASIP Journal on Wireless Communications and Networking, vol. 2018, 12 2018.

[12] G. Castellanos, M. Deruyck, L. Martens, and W. Joseph, "Performance evaluation of direct-link backhaul for uav-aided emergency networks," Sensors, vol. 19, no. 15, p. 3342, 2019.

[13] M. Mozaffari, W. Saad, M. Bennis, Y.-H. Nam, and M. Debbah, "A tutorial on uavs for wireless networks: Applications, challenges, and open problems," IEEE communications surveys & tutorials, vol. 21, no. 3, pp. 2334–2360, 2019.

[14] Q. Wu, L. Liu, and R. Zhang, "Fundamental trade-offs in communication and trajectory design for uav-enabled wireless network," IEEE Wireless Communications, vol. 26, no. 1, pp. 36–44, 2019.

[15] M. Deruyck, A. Marri, S. Mignardi, L. Martens, W. Joseph, and R. Verdone, "Performance evaluation of the dynamic trajectory design for an unmanned aerial base station in a single frequency network," in 2017 IEEE 28th Annual International Symposium on Personal, Indoor, and Mobile Radio Communications (PIMRC), pp. 1–7, IEEE, 2017.

[16] A. V. Savkin and H. Huang, "Deployment of unmanned aerial vehicle base stations for optimal quality of coverage," IEEE Wireless Communications Letters, vol. 8, no. 1, pp. 321–324, 2018.

[17] H. Huang and A. V. Savkin, "A method for optimized deployment of unmanned aerial vehicles for maximum coverage and minimum interference in cellular networks," IEEE Transactions on Industrial Informatics, vol. 15, no. 5, pp. 2638–2647, 2018.

[18] C. T. Cicek, H. Gultekin, B. Tavli, and H. Yanikomeroglu, "Uav base station location optimization for next generation wireless networks: Overview and future research directions," in 2019 1st International Conference on Unmanned Vehicle Systems-Oman (UVS), pp. 1–6, IEEE, 2019.

[19] M. Deruyck, E. Tanghe, D. Plets, L. Martens, and W. Joseph, "Optimizing lte wireless access networks towards power consumption and electromagnetic exposure of human beings," Computer Networks, vol. 94, 12 2015.

[20] A. Rizwan, D. Biswas, and V. Ramachandra, "Impact of uav structure on antenna radiation patterns at different frequencies," in 2017 IEEE International Conference on Antenna Innovations & Modern Technologies for Ground, Aircraft and Satellite Applications (iAIM), pp. 1–5, IEEE, 2017.

[21] M. Nosrati, A. Jafargholi, and N. Tavassolian, "A broadband blade dipole antenna for uav applications," in 2016 IEEE International Symposium on Antennas and Propagation (APSURSI), pp. 1777–1778, IEEE, 2016.

[22] M. Nosrati, A. Jafargholi, R. Pazoki, and N. Tavassolian, "Broadband slotted blade dipole antenna for airborne uav applications," IEEE Transactions on Antennas and Propagation, vol. 66, no. 8, pp. 3857–3864, 2018.

[23] B. A. Arand, R. Shamsaee, and B. Yektakhah, "Design and fabrication of a broadband blade monopole antenna operating in 30 mhz–600 mhz frequency band," in 2013 21st Iranian Conference on Electrical Engineering (ICEE), pp. 1–3, IEEE, 2013.

[24] L. Akhoondzadeh-Asl, J. Hill, J.-J. Laurin, and M. Riel, "Novel low profile wideband monopole antenna for avionics applications," IEEE transactions on antennas and propagation, vol. 61, no. 11, pp. 5766–5770, 2013.

[25] S. S. Siddiq, G. Karthikeya, T. Tanjavur, and N. Agnihotri, "Microstrip dual band millimeter-wave antenna array for uav applications," in 2016 21st International Conference on Microwave, Radar and Wireless Communications (MIKON), pp. 1–4, IEEE, 2016.

[26] Y. Zheng, J. Zhou, W. Wang, and M. Chen, "A low-profile broadband circularly polarized antenna array for uav ground-to-air communication," in 2018 IEEE Asia-Pacific Conference on Antennas and Propagation (APCAP), pp. 219–220, IEEE, 2018.

[27] X. Sun, R. Blázquez-García, A. García-Tejero, J. M. Fernández-González, M. Burgos-García, and M. Sierra-Castañer, "Circular array antenna tor uav-uav communications," in 2017 11th European Conference on Antennas and Propagation (EUCAP), pp. 2025–2028, IEEE, 2017.

[28] I. Singh and V. Tripathi, "Micro strip patch antenna and its applications: a survey," Int. J. Comp. Tech. Appl, vol. 2, no. 5, pp. 1595–1599, 2011.

[29] K. Kashwan, V. Rajeshkumar, T. Gunasekaran, and K. S. Kumar, "Design and characterization of pin fed microstrip patch antennae," in 2011 Eighth International Conference on Fuzzy Systems and Knowledge Discovery (FSKD), vol. 4, pp. 2258–2262, IEEE, 2011.